Published in final edited form as:
Biochemistry. 2013 October 8; 52(40): 7082–7090. doi:10.1021/bi400678y.

Identification of novel integrin binding partners for CIB1: structural and thermodynamic basis of CIB1 promiscuity

Thomas C. Freeman Jr.[1], **Justin L. Black**[1], **Holly G. Bray**[1], **Onur Dagliyan**[1], **Yi I. Wu**[1,†], **Ashutosh Tripathy**[1], **Nikolay V. Dokholyan**[1,2], **Tina M. Leisner**[1,‡], and **Leslie V. Parise**[1,2,3,‡,*]

[1]Department of Biochemistry and Biophysics, School of Medicine, University of North Carolina, Chapel Hill, NC 27599

[2]Lineberger Comprehensive Cancer Center, School of Medicine, University of North Carolina, Chapel Hill, NC 27599

[3]McAllister Heart Institute, School of Medicine, University of North Carolina, Chapel Hill, NC 27599

Abstract

The short cytoplasmic tails of the α and β chains of integrin adhesion receptors regulate integrin activation and cell signaling. Significantly less is known about proteins that bind to α-integrin cytoplasmic tails (CTs) than β-CTs to regulate integrins. CIB1 was previously identified as an αIIb binding partner that inhibits agonist-induced activation of the platelet-specific integrin, αIIbβ3. A sequence alignment of all α-integrin CTs revealed that key residues in the CIB1 binding site on αIIb are well-conserved, and was used to delineate a consensus binding site (I/L-x-x-x-L/M-W/Y-K-x-G-F-F). Because the CIB1 binding site on αIIb is conserved in all α-integrins, and CIB1 expression is ubiquitous, we asked if CIB1 could interact with other α-integrin CTs. We predicted that multiple α-integrin CTs were capable of binding to the same hydrophobic binding pocket on CIB1 with docking models generated by all-atom replica exchange discrete molecular dynamics. After demonstrating novel *in vivo* interactions between CIB1 and other whole integrin complexes with co-immunopreceipitations, we validated the modeled predictions with solid-phase competitive binding assays showing that other α-integrin CTs compete with the αIIb CT for binding to CIB1 *in vitro*. Isothermal titration calorimetry measurements indicated that this binding is driven by hydrophobic interactions and depends on residues in the CIB1 consensus binding site. These new mechanistic details of CIB1-integrin binding imply that CIB1 could bind to all integrin complexes and act as a broad regulator of integrin function.

[*]To whom correspondence should be addressed: Department of Biochemistry and Biophysics, 3016 Genetic Medicine CB#7260, 120 Mason Farm Road, University of North Carolina at Chapel Hill, Chapel Hill, NC 27599-7260, Tel: 919-966-2238, Fax: 919-966-2852, leslie_parise@med.unc.edu.
[†]Present address is UConn Health Center, Center for Cell Analysis and Modeling, Cell and Genome Sciences Building, MC 6406 400 Farmington Avenue, Farmington, CT 06030
[‡]Co-senior authors.

Supporting Information Available: Figures of an alignment of all α-integrin cytoplasmic tails and ITC titration isotherms, and a table showing the sequences of all tested α-integrin CT peptides are included in the supporting information. This material is available free of charge via the Internet at http://pubs.acs.org.

INTRODUCTION

Integrins are a large family of heterodimeric (α/β) transmembrane proteins found in almost every mammalian cell type. This family consists of 18 α-subunits and 8 β-subunits that can pair to form 24 different heterodimers. These proteins control many normal cellular processes including migration, growth, differentiation, and proliferation (1). Integrins also play significant roles in many diseases including Glanzmann's thrombasthenia, various immune disorders, and cancer (2-4). Therefore, examining the details of integrin regulation and signaling is essential.

A better understanding of the protein-protein interactions occurring at the integrin cytoplasmic tails (CTs) is necessary to elucidate the details of bidirectional integrin signaling. While there are well-understood integrin β-subunit binding proteins like talin, the kindlins, Rab25, PKCα, Src, Numb, and many others (5, 6), there are many fewer known α-subunit binding partners *e.g.* Nischarin, Calreticulin, Rab21, p120RasGAP, SHARPIN, and GIPC1(7-11). We previously reported CIB1 (calcium and integrin binding protein 1) as a binding partner for the αIIb CT of the platelet-specific αIIbβ3 integrin (12).

CIB1 is a 22 kDa, helical, EF-hand-containing protein related to calcineurin B, and is expressed in many cell types (13-17). Previous studies revealed that highly conserved residues N-terminal to the GFFKR motif of the αIIb CT were essential for CIB1 binding (13, 18). Additionally, multiple reports indicate that CIB1 may modulate either inside-out (19) or outside-in (20, 21) αIIbβ3 signaling. Besides αIIb, CIB1 binds to a variety of other proteins including signaling proteins PAK1, Snk, and Fnk (22, 23). While CIB1 is not required for normal embryonic development (24), potentially because of compensation by CIB family members CIB2, CIB3, and/or CIB4 (25), CIB1 knockout mice exhibit phenotypic abnormalities, including impaired pathological angiogenesis, reduced tumor growth, protection from cardiac hypertrophy, and male sterility (24, 26-28). Here we examined the physical relationship of the CIB1-integrin interaction in order to gain more insight into the functional roles of CIB1.

Because CIB1 binds to a conserved region on αIIb, and is ubiquitously expressed, we hypothesized that CIB1 may bind to other α-integrin CTs. We used molecular docking simulations to test the plausibility of our hypothesis, and found that αIIb, α5, and αV cytoplasmic tail peptides dock to the same hydrophobic binding pocket on CIB1. We show that CIB1 binds to αVβ3 and α5β1 integrins in mammalian cells via co-immunoprecipitation, demonstrating that CIB1 can interact with different whole integrin complexes *in vivo*. We also found that the CT peptides of many integrins, which included representative members of each receptor subfamily, compete with αIIb for binding to CIB1. Further, we show that CIB1 binding to all tested α-integrin peptides is driven by hydrophobic interactions, and that there is a correlation between the hydrophobicity of the CIB1 binding site on α-integrin CT peptides and binding affinity. These findings indicate that CIB1 is an even more versatile integrin binding protein than previously realized, and suggest that CIB1 may play a common role with different integrins.

EXPERIMENTAL PROCEDURES

Protein purification and peptide synthesis

Human wild type CIB1 was cloned into pProEX HTc (Invitrogen), and further modified to include an upstream amino-terminal hexahistadine tag followed by a tobacco etch virus (TEV) cleavage site to facilitate removal of the hexahistadine tag. CIB1 mutants ^{114}IFDF/AADA, ^{152}LI/AA, and ^{173}F/A were made as previously described (18). Mutant and WT CIB1 was expressed and purified from *E. coli* BL21(DE3) as described previously with slight modifications as follows (14). After harvesting the cells, lysing by sonication, and centrifugation, clarified cell lysate was loaded onto an AKTA Purifier UPC 100 fitted with a 20 mL His-Prep FF 16/10 column (GE Healthcare). Fractions containing CIB1 were pooled and dialyzed in storage buffer (50 mM HEPES (pH 7.4), 150 mM NaCl, 10% (v/v) glycerol, and 100 μM $CaCl_2$). The 6xHis tag was removed by proteolysis using His-tagged TEV, which was added at approximately 1 mg/100 mg of CIB1 along with 1 mM DTT, and 0.5 mM EDTA. Cleavage was carried out overnight at room temperature. Mature CIB1 was isolated by subtractive Ni^{2+} affinity purification, where His-TEV was bound to the column, and CIB1 was collected in the flowthru. The DTT and EDTA was removed by dialysis in storage buffer. Protein concentration of mature CIB1 was measured by absorbance at 280 nm and $\varepsilon = 2980\ cm^{-1}\ M^{-1}$.

Peptides were synthesized by either Bio-Synthesis, Inc. or via the High-Throughput Peptide Core and Arraying Facility at UNC-CH and purified by high performance liquid chromatography (HPLC). Peptide mass was confirmed by MALDI MS/MS on a 7400 Proteomics Analyzer (Applied Biosystems). Sequences used are listed in Table S1.

To generate cytoplasmic tails that could be precipitated with amylose resin beads, DNA encoding either residues 1014-1039 of human wild type αIIb, or residues 1011-1048 of human wild type αV was cloned into a pMAL vector (New England Biosystems) downstream of the *malE* gene. The fusion protein-encoding vectors were transformed into *E. coli* BL21Star(DE3), which were then grown at 37°C in 1 L of LB, and 1mM IPTG was added to induce over-expression of the MBP-α-integrin CT fusion proteins, which continued for 4 hours at 37°C. The cultures were harvested by centrifugation, resuspended in 50 mM HEPES (pH 7.4), 150 mM NaCl, lysed by sonication, and then clarified by centrifugation. The MBP fusion products were purified from the lysates amylose resin beads (New England Biolabs) according to the manufacturer's instructions. Samples were dialyzed against 50 mM HEPES (pH 7.4), 150 mM NaCl, 10% (v/v) glycerol overnight, tested for purity by SDS PAGE, and final protein concentration was measured using the BCA protein assay (Pierce).

All-atom replica exchange discrete molecular dynamics (DMD)

Modeling of CIB1 binding to α5 and αV cytoplasmic tail peptides was performed to test for potential binding interactions with CIB1, and those models were compared to a simulation of αIIb binding to CIB1. The model of CIB1 used in the simulations was either a homology model of CIB1 based on the ligand-bound form of calcineurin B (PDB code: 1DGU) or the solution structure of αIIb-CT-bound CIB1 (PDB code: 2LM5) (29). The structure of αIIb

was taken from (PDB code: 2KNC), and α5 and αV peptide structures were modeled after the αIIb structure using I-TASSER (30, 31). The starting structure of each integrin peptide was placed approximately 40 Å away from CIB1 using the edit functions of PyMol (32). The DMD simulations were performed as described by Dagliyan, *et al.* (33). In these simulations the backbone of CIB1 was fixed while all atoms of the peptides were free to move with some constraints added to preserve the secondary structure. The DMD engine approximates inter-atomic interactions by discrete square well potentials, and models proteins using the united atom representation. The Van der Waals forces, solvation interactions, and electrostatic interactions are modeled in a discretized manner as well. In replica exchange, a simulation is performed in replicate at different temperatures and the structures are exchanged between the replicates at regular intervals. This robust approach allows the engine to more easily overcome energy barriers. The length of each simulation was 10^6 time units, which is approximately 50 ns of real time. After the DMD simulations were complete, hierarchical clustering of the integrin-binding conformations, or poses representing a single instantaneous posture captured during the simulation, were performed using root-mean-square distances (RMSD) calculated over all heavy atoms in the peptide, and MedusaScore was used to evaluate the energy landscape of the clustered poses (34). The lowest energy complexes were taken from the largest clusters and further refined using MedusaDock to obtain the final structures (35). Images of the models were created using PyMol. Atom pair contacts made between CIB1 and the integrin CT peptides were identified in the docking models by finding all residues on CIB1 that were within 4 Å of any side chain atom on the integrin CT peptide using PyMol.

Co-immunoprecipitation (co-IP)

Co-IP was performed to determine whether CIB1 associates with αVβ3 or α5β1 integrin complexes in mammalian cells as previously described with some modifications (19). HEK29-T cells were maintained in DMEM supplemented with 10% FBS and 1% non-essential amino acids at 37°C and 5% CO_2. Plasmids encoding human integrin α5 or αV were transiently transfected in HEK293T cells using Fugene (Roche) according to manufacturer's instructions. Cells were harvested and lysed with CHAPS lysis buffer (25 mM HEPES [pH 7.4], 150 mM NaCl, 10 mM CHAPS, 30 mM NaF, 10 mM β-glycerophosphate, 0.2 mM Na_3VO_4, 1.25 mg/mL N-ethylmaleimide, 0.1 mM $CaCl_2$, 0.1 mM $MgCl_2$, 5% glycerol, and Protease Inhibitor Cocktail III (Calbiochem) diluted 1:100). Clarified lysates were incubated overnight with either chicken non-specific or anti-CIB1 IgY, and immune complexes were precipitated using goat anti-chicken IgY agarose beads (Aves Labs, Inc.). Beads were washed three times in lysis buffer and eluted with 1X non-reducing sample buffer. Samples were resolved by SDS-PAGE, transferred to PDVF membrane and immunoblotted with rabbit anti-integrin α5 polyclonal antibody (Millipore), mouse anti-integrin αV monoclonal antibody (BD Transduction) or chicken anti-human CIB1 IgY.

Co-precipitation assay

Purified recombinant MBP-αIIb or MBP-αV cytoplasmic tails were loaded onto amylose resin beads and washed 3x in assay buffer (25 mM HEPES, pH 7.4, 150 mM NaCl, 0.1 mM $CaCl_2$). MBP-tail beads were added to recombinant WT or mutant CIB1 proteins diluted in

assay buffer (0.75 mg/ml) and incubated 1 h at 4°C. Beads were washed 3x with assay buffer and samples were analyzed by SDS-PAGE.

Solid-phase binding assays

Competitive inhibition solid-phase binding assays were performed to measure CIB1 binding to multiple α-integrin cytoplasmic tail (CT) peptides. Various α-integrin CT peptides were immobilized in 96-well plates. Increasing concentrations of soluble peptides were used to compete with the immobilized peptide for CIB1 binding. Immulon 1B 96-well plates (Fisher Scientific) were coated with 50 μL of 50 μM peptide solutions, which were incubated overnight at room temperature (all subsequent incubations were performed at room temperature). Empty and peptide-coated wells were blocked with 3% BSA (bovine serum albumin) in PBS (phosphate-buffered saline). CIB1 (between 0.05 and 0.1 μM final concentrations) was mixed with various concentrations of soluble peptide in 50 mM HEPES (pH 7.4), 150 mM NaCl, 0.1 mM $CaCl_2$, 0.1 mM $MgCl_2$, and added to microtiter wells in a final volume of 50 μL/well. Solutions were discarded and the wells were washed thrice with 200 μL of 0.05% Tween in Tris-buffered saline, pH 7.4 (TBS-T); all subsequent incubations were preceded by similar washing steps. To detect CIB1 binding, chicken anti-CIB1-IgY was added and incubated 1 h followed by addition of HRP-conjugated donkey anti-chicken - IgG (Jackson ImmunoResearch). To visualize antibody binding, Sigma*FAST o*-phenylenediamine (OPD) solution (Sigma) was added and the reaction allowed to proceed for at least 10 min. The reaction was terminated by addition of 4N H_2SO_4 and absorbance was measured at 490 nm in a 96-well microplate reader (Spectramax M5).

Isothermal titration calorimetry (ITC)

ITC was performed to quantify the thermodynamics of binding between CIB1 and α-integrin tail peptides as previously described with minor modifications (13). Purified CIB1 was dialyzed extensively in 50 mM HEPES (pH 7.4), 150 mM NaCl, 0.1 mM $CaCl_2$ (unless noted differently elsewhere), and diluted to a concentration of 100 μM. Peptides were freshly dissolved to concentrations ranging from 0.8 to 1 mM in the same buffer as CIB1. Isothermal titrations were performed using a MicroCal VPITC microcalorimeter. Injections of 10 μL of peptide were added at 300 s intervals at either 15° C or 26° C. The heats of dilution were estimated from injections made after saturation occurred. These values were subtracted from the data before one-site curve fitting was performed using Microcal, LLD Origin 7. The stoichiometry (*N*), association and dissociation constants (K_a, K_d), and enthalpy change (ΔH) were obtained directly from the data, and the Gibbs free energy change (ΔG) and entropy change (ΔS) were calculated by Equations 1 - 3.

$$\Delta G = \Delta H - T\Delta S \quad (1)$$

$$\Delta G = -RTlnK_a \quad (2)$$

$$K_d = 1/K_a \quad (3)$$

RESULTS

Sequence conservation of α-integrin cytoplasmic tails (CTs)

The C-terminal sequences of several α-integrin subunits were aligned to assess the likelihood that CIB1 could bind to other integrins besides αIIb. The alignment in Fig. 1 shows several highly conserved residues in the membrane-proximal region of the integrin tails, revealing a consensus motif of I/L-x-x-x-L/M-W/Y-K-x-G-F-F. The consensus sequence is conserved in all 18 α-integrin CTs (Fig. S1). This observation led us to hypothesize that CIB1 can bind to most other integrins, and potentially contribute to their signaling pathways. Each α-integrin CT shown in Fig. 1 was tested for binding to CIB1. We selected a functionally diverse subset of α-integrins that included αV, the only other β3 integrin partner, the ubiquitous fibronectin receptor, α5, which binds to the R-G-D sequence, and some commonly observed representatives from other receptor subclasses; a laminin receptor (α3), a collagen receptor (α2), leukocyte-specific receptors (αM and αL), and a non-RGD fibronectin receptor (α4) (1).

Docking of α-integrin CTs to CIB1

We attempted to identify the most likely integrin binding site on CIB1 using replica-exchange discrete molecular dynamics (DMD) simulations (Fig. 2A). The starting CIB1 structure, a homology model to Calcineurin B (PDB code 1DGU), was chosen because it has the C-terminal helix of CIB1 displaced, which is a key mechanism in integrin binding by CIB1 (36, 37). This model of CIB1 was sufficient for the purposes of qualitatively assessing the likelihood of CIB1 interacting with multiple integrins. Representatives of the most frequently sampled conformations from the lowest energy clusters of these simulations indicate a significant overlap in the binding sites occupied on CIB1 by each α-integrin CT tested (Fig. 2B). Furthermore, the integrin residues that were close enough to contact CIB1 included at least the first three N-terminal hydrophobic residues of each integrin peptide. The GFFKR motifs were only involved in the binding interfaces of αIIb and αV, with both $Phe^{1023\text{-}1024}$ residues in αIIb contacting CIB1, and only Phe^{1020} of αV making contact. As a consequence of the sequence variation of the α-integrin CTs and the randomized sampling of the simulation, the number of atom pair contacts formed between CIB1 and each α-integrin CT varied; αIIb, α5, and αV appeared to contact 9, 5, and 12 residues on CIB1 respectively.

Association of CIB1 with αVβ3 and α5β1 integrins in mammalian cells

Because we predicted that CIB1 could bind to α5 and αV integrins in simulations, we asked if we could detect CIB1 binding to integrins in cells via co-immunoprecipitation assays. Endogenous CIB1 was immunoprecipitated from HEK293T cells overexpressing either integrin α5 or integrin αV (Fig. 2C), and both integrins co-precipitated with CIB1.

Competitive binding of α-integrin CT peptides to αIIb binding site of CIB1

Because molecular docking suggests that α5 and αV peptides can bind to sites overlapping that of αIIb, we tested the ability of various α-integrin CTs (see Table S1) to compete with αIIb CT peptide for CIB1 binding in competitive solid-phase binding assays. Most solution-

phase integrin peptides dose-dependently inhibited CIB1 binding to αIIb CT peptide (Fig. 2D). The IC_{50} ± 95% CI of αIIb, α2, α5, αL, and αV was 9.6 ± 1.1, 6.0 ± 4.0, 8.3 ± 1.3, 19.7 ± 6.7, and 2.7 ± 1.3 respectively. The relatively weak competitive inhibition of CIB1 binding by αM, α3, and α4 CT peptides was not sufficient to determine IC_{50} values.

Effect of integrin N-terminal CT residues on CIB1 binding

Previous data show that the hydrophobic N-terminal residues on the αIIb CT peptide are important for binding to CIB1 (18). We therefore asked if changing residues in this region of αV would similarly disrupt binding to CIB1. CIB1 binding to αV peptides with either four or six alanine substitutions at the N-terminus (αV-4A, and αV-6A respectively) was compared to CIB1 binding to αV-WT via ITC (Fig. 3A-C). While αV-WT binds to CIB1 endothermically with a 1:1 stoichiometry and a K_d of 4.3 μM, isothermal data for αV-4A and αV-6A appear to have been generated solely from heats of dilution of the peptides, and we could not reliably fit these data to any standard binding models.

Effect of mutating residues in CIB1 hydrophobic pocket on integrin-binding

We used previously generated CIB1 mutants shown to inhibit binding to αIIb to determine if these mutations could also inhibit binding of different integrins (18). These mutated residues are also a part of the hydrophobic binding surface on CIB1, and formed atom pair contacts with the integrin peptides in the docking simulations. We tested binding of CIB1 mutants, ^{152}LI/AA, ^{114}IFDF/AADA, and ^{173}F/A to fusion proteins, MBP-αIIb CT and MBP-αV CT (Fig. 3D). The western blots show that all tested CIB1 mutations differentially affect binding to distinct integrins. Notably, mutation of CIB1 residues ^{152}LI/AA and ^{173}F/A significantly reduced CIB1 binding to the αIIb CT fusion protein, whereas mutation of ^{114}IFDF/AADA residues significantly reduced binding to the αV CT fusion protein.

The role of hydrophobic interactions in CIB1 binding to α-integrins

To further characterize the mechanism of binding between CIB1 and α-integrin CTs, we used isothermal titration calorimetry (ITC) to measure the binding thermodynamics between CIB1 and additional α-integrin CT peptides. The binding data show a stoichiometry of 1:1 with μM binding affinities between CIB1 and all α-integrin peptides tested (Table 1, Fig. S2), which is consistent with previously measured binding affinities between CIB1 and αIIb (13, 38-40). In contrast to the competitive ELISA results where neither α3 nor αM competed effectively with immobilized αIIb for CIB1 binding (Fig. 2D), ITC results indicated that the α3 and αM CT peptides do bind CIB1, albeit with significantly lower affinities than αIIb. While the binding affinities of the weakest CIB1-binding peptide and the strongest vary by an order of magnitude, the thermodynamic characteristics are similar. With the exception of the exothermic binding exhibited by CIB1 binding to the αIIb CT peptide, CIB1 binding to all other peptides was endothermic. The thermodynamic profiles of CIB1 binding to the various α-integrin CT peptides suggest that the CIB1-integrin interaction is mainly driven by hydrophobic interactions (Fig. 4A) (41). Overall, CIB1 bound to α-integrin CTs with similar stoichiometry, affinity, free energy, and entropy.

Correlation between hydrophobicity of N-terminal CT amino acids and CIB1-integrin binding affinity

We reexamined the α-integrin peptide sequences to identify potential factors that may explain why there was some variance in CIB1 binding thermodynamics, and determined that the most sequence variance within the CIB1 binding region occurred among the N-terminal residues (Fig. 4B). Given the potential variability in CIB1-integrin atom-pair contacts and an apparently dominant role played by hydrophobic interactions in CIB1-integrin binding, we asked if there was a relationship between the hydrophobicity of the N-terminal membrane proximal region of the integrins and CIB1 binding affinity. We used the empirically-defined Wimley-White water-octanol scale (where more negative values indicate greater hydrophobicity) to calculate the total side-chain hydrophobicity of the highly varied membrane-proximal residues (the second through fourth residues) of each α-integrin CT peptide tested (42). Linear regression of the data reveal a negative correlation between the total hydrophobicity of the highly varied region of the α-integrin peptides and the CIB1 binding affinity measured by ITC, with a slope of −1.7 ± 0.5 and $R^2 = 0.72$ (Fig. 4B). The calculated hydrophobicities in the highly varied region of all α-integrin CTs are within the range (−3.62 to +1.25 kcal/mol) of the tested set of α-integrin CTs (Fig. 4C).

DISCUSSION

Because integrin function is regulated by cytoplasmic tail-binding proteins, and the potential regulatory roles played by α-integrin binding proteins have been less studied than β-integrin binding proteins, we explored the α-integrin binding capabilities of CIB1. CIB1 is ubiquitously expressed, and interacts with a region of the platelet-specific integrin αIIb cytoplasmic tail that is well-conserved in all α-integrins. These observations suggested that CIB1 can bind to other α-integrins.

To quickly assess the feasibility of testing the hypothesis that CIB1 binds to other α-integrin CTs, we used discrete molecular dynamics (DMD) simulations, which have been successfully employed in various capacities to obtain accurate estimates of protein-peptide interactions using only structural data of the receptor and ligand as input (33, 43). The docking simulations showed structural details of CIB1 binding to αIIb, α5, and αV CT peptides, and a comparison to the recent CIB1-αIIb complex structure (15) validated that these simulations produced plausible models. The interaction interface predicted by the docking simulations was supported by mutational analysis where CIB1 mutants in the hydrophobic binding surface selectively affected binding to different integrins, and Ala substitutions in integrin peptides disrupted binding to CIB1. The positive results from the simulations not only suggested that CIB1 can bind to multiple α-integrins, but that multiple integrins bind to the expected hydrophobic surface on CIB1. This result led us to test whether or not CIB1 could actually bind to multiple integrins in cells. We therefore co-immunoprecipitated whole integrins; the results validated that CIB1 can bind to other integrins in cells, as it does αIIbβ3 (13). Furthermore, competitive binding experiments showed that several α-integrin CT peptides compete with the αIIb CT for CIB1 binding, which supported the simulation data that integrins bind to the same general region on CIB1. Interestingly, integrins α3, αM, and α4, which have sequences least similar to αIIb,

competed poorly with αIIb for CIB1 binding. As expected, ITC measurements showed that the binding affinity of αM may not be strong enough to compete with αIIb under the tested conditions. In contrast, the CIB1 binding affinities for α3 and α4 are likely strong enough to compete with αIIb, if competition is for the same binding site. This supports a possibility raised by docking simulations that different integrins may bind to different local binding sites within the same pocket on CIB1. Further, the possibility of integrins binding to different binding sites within the hydrophobic binding pocket of CIB1 was supported by *in vitro* co-precipitation assays using various CIB1 mutants and MBP-integrin CT fusion proteins. Three different sets of CIB1 mutations differentially affected CIB1 binding to two different α-integrins, suggesting that while integrins may bind within the same binding pocket, the specific molecular contacts are different. Furthermore, mutations in CIB1 around the Mg^{2+}/Ca^{2+} binding site in EF-hand III that were previously shown not to affect αIIb binding (44), did affect αV binding. This localized specificity may explain how CIB1 is able to bind to many different integrins using the same binding pocket. This dynamic binding capacity of CIB1 may also be heavily influenced *in vivo* by Mg^{2+} and Ca^{2+} concentrations, which have dramatic effects on CIB1 structure and binding affinity (16, 36, 37, 40, 44).

In addition to identifying the integrin-binding site on CIB1, we also validated that the highly conserved membrane-proximal region of α-integrin CTs is the CIB1 binding site. Substituting alanine residues for a series of N-terminal residues in the αV CT peptide abolished binding to CIB1, which is in agreement with previous reports that these residues are important for CIB1 binding to αIIb (18). We can therefore infer that these hydrophobic residues in the consensus binding sequence are essential for CIB1 binding to all α-integrin CTs. Moreover, we have shown that there is a correlation between the total side-chain hydrophobicity of residues in this region and CIB1 binding affinity. Even though binding affinity increases as the total side-chain hydrophobicity in this region decreases, the least hydrophobic peptide, αM, had the weakest binding affinity. This indicates that an optimum range of hydrophobicities of these residues coincides with a stronger binding affinity to CIB1. Based on this observed relationship, we calculated the hydrophobicities of the highly varied region of the consensus motif in all α-integrins. Because the test set includes representative members of each integrin subfamily, and all of the calculated hydrophobicities fall within the range of the tested integrins, we conclude that the strength of CIB1 binding to all α-integrins can be categorized as moderate if the highly varied region is hydrophobic or weak if this region is hydrophilic. These hydrophobicity data do not, however, explain why αIIb exhibits exothermic binding, while the other peptides exhibit endothermic binding. We suspect that the Ala in the fourth position of the αIIb peptide is necessary, but not sufficient to cause this difference in enthalpy. This is evidenced in part by the Ala substitutions made in the αV peptides where the enthalpy of binding to CIB1 goes from endothermic with the WT peptide to exothermic with the 4-Ala peptide. We believe that this is not sufficient, however, because αM, which has an Ala in the same position exhibits endothermic binding. Further testing is required to clarify how the integrin sequence affects the thermodynamic properties of binding to CIB1.

To gain greater insight into the binding mechanism and biological potential of CIB1, we measured the binding thermodynamics between CIB1 and several α-integrin CT peptides.

We were surprised to find that the enthalpies of binding between CIB1 and the newly tested α-integrin sequences differed from that of αIIb, yet the binding affinities were relatively similar to one another. This may indicate that there is an αIIb-specific binding mechanism, which begs the question of whether different binding mechanisms correlate with different functional roles. Previous evidence indicated that CIB1 plays a role in inside-out integrin signaling by negatively regulating αIIbβ3 activation in thrombin-stimulated megakaryocytes (19), and contributes to outside-in signaling by regulating cell spreading through focal adhesion kinase (FAK) (20, 21). Whether CIB1 plays similar roles with other integrins, or different roles, as potentially implied by its distinct thermodynamic binding properties with other integrins, is currently unknown but will be of interest for future studies.

In conclusion, we present data that CIB1 binds to seven additional α-integrin CT peptides, bringing the total number of α-integrins that can associate with CIB1 to eight. Because some α-integrins may form heterodimers with multiple β-integrins (*e.g.*, αVβ1, αVβ3), we infer that the total number of integrin complexes with which CIB1 interacts is 13. Based on sequence comparisons of the cytoplasmic membrane-proximal regions of the remaining 10 α-integrin subunits, we predict that CIB1 could bind to all 24 known integrin heterodimers. These findings suggests that CIB1 may be a much broader regulator of integrin function than previously realized. Additionally, broad integrin-binding activity is potentially conserved across CIB family proteins as indicated by the finding that CIB2 binds to α7 and αIIb (45, 46). Because this study suggests that CIB1 may act as a broad regulator of integrin function, and recent evidence revealed that CIB1 plays a vital role in cancer cell survival (47), it is important to further investigate mechanistic and functional details of CIB1-integrin interactions.

Supplementary Material

Refer to Web version on PubMed Central for supplementary material.

Acknowledgments

Thanks to Feng Ding for assistance in computational modeling. We also thank Jun Qin of the Cleveland Clinic for many helpful discussions and early insights. Onur Dagliyan is a Howard Hughes Medical Institute International Student Research Fellow.

Funding Sources: This work was supported by R01 HL092544 to LVP, R21 NS071216 to YIW, RO1 GM080742 to NVD, and TCF was supported through the NIGMS IRACDA program 5K12-GM000678.

Abbreviations

BCA	Bicinchronic Acid
CIB1	Calcium-and-Integrin-Binding protein 1
Co-IP	Co-Immunoprecipitation
CT	Cytoplasmic Tail
DMD	Discrete Molecular Dynamics
ELISA	Enzyme-linked Immunosorbant Assay

FAK	Focal Adhesion Kinase
GAIP	Gα-interacting protein
GIPC1	GAIP C-terminus interacting protein 1
HEK293T	Human Embryonic Kidney 293 Temperature-sensitive cells
HEPES	4-(2-hydroxyethyl)piperazine-1-ethanesulfonic acid
HB	Hydrogen Bonding
HI	Hydrophobic Interactions
ITC	Isothermal Titration Calorimetry
LB	Luria-Bertani Broth
MBP	Maltose Binding Protein
PAK1	p21 Activated Kinase 1
PBS	Phosphte-Buffered Saline
RH	regulator of G protein signaling homology
SDS-PAGE	Sodium Dodecyl Sulfate-Polyacrylamide Gel Electrophoresis
SHARPIN	Shank-associated RH domain interactor
TEV	Tobacco Etch Virus protease

REFERENCES

1. Hynes RO. Integrins: bidirectional, allosteric signaling machines. Cell. 2002; 110:673–687. [PubMed: 12297042]
2. Felding-Habermann B. Integrin adhesion receptors in tumor metastasis. Clin Exp Metastasis. 2003; 20:203–213. [PubMed: 12741679]
3. Kato A. The biologic and clinical spectrum of Glanzmann's thrombasthenia: implications of integrin alpha IIb beta - for its pathogenesis. Crit Rev Oncol Hematol. 1997; 26:1–23. [PubMed: 9246538]
4. Yonekawa K, Harlan JM. Targeting leukocyte integrins in human diseases. J Leukoc Biol. 2005; 77:129–140. [PubMed: 15548573]
5. Knezevic I, Leisner TM, Lam SC. Direct binding of the platelet integrin alphaIIbbeta3 (GPIIb-IIIa) to talin. Evidence that interaction is mediated through the cytoplasmic domains of both alphaIIb and beta3. J Biol Chem. 1996; 271:16416–16421. [PubMed: 8663236]
6. Moser M, Nieswandt B, Ussar S, Pozgajova M, Fassler R. Kindlin-3 is essential for integrin activation and platelet aggregation. Nat Med. 2008; 14:325–330. [PubMed: 18278053]
7. Rantala JK, Pouwels J, Pellinen T, Veltel S, Laasola P, Mattila E, Potter CS, Duffy T, Sundberg JP, Kallioniemi O, Askari JA, Humphries MJ, Parsons M, Salmi M, Ivaska J. SHARPIN is an endogenous inhibitor of beta1-integrin activation. Nat Cell Biol. 2011; 13:1315–1324. [PubMed: 21947080]
8. Mai A, Veltel S, Pellinen T, Padzik A, Coffey E, Marjomaki V, Ivaska J. Competitive binding of Rab21 and p120RasGAP to integrins regulates receptor traffic and migration. J Cell Biol. 2011; 194:291–306. [PubMed: 21768288]
9. Valdembri D, Caswell PT, Anderson KI, Schwarz JP, Konig I, Astanina E, Caccavari F, Norman JC, Humphries MJ, Bussolino F, Serini G. Neuropilin-1/GIPC1 signaling regulates alpha5beta1 integrin traffic and function in endothelial cells. PLoS Biol. 2009; 7:e25. [PubMed: 19175293]

10. Alahari SK, Nasrallah H. A membrane proximal region of the integrin alpha5 subunit is important for its interaction with nischarin. Biochem J. 2004; 377:449–457. [PubMed: 14535848]
11. Coppolino M, Leung-Hagesteijn C, Dedhar S, Wilkins J. Inducible interaction of integrin alpha 2 beta 1 with calreticulin. Dependence on the activation state of the integrin. J Biol Chem. 1995; 270:23132–23138. [PubMed: 7559457]
12. Naik UP, Patel PM, Parise LV. Identification of a novel calcium-binding protein that interacts with the integrin alphaIIb cytoplasmic domain. J.Biol.Chem. 1997; 272:4651–4654. [PubMed: 9030514]
13. Shock DD, Naik UP, Brittain JE, Alahari SK, Sondek J, Parise LV. Calcium-dependent properties of CIB binding to the integrin alphaIIb cytoplasmic domain and translocation to the platelet cytoskeleton. Biochem.J. 1999; 342(Pt 3):729–735. [PubMed: 10477286]
14. Gentry HR, Singer AU, Betts L, Yang C, Ferrara JD, Sondek J, Parise LV. Structural and biochemical characterization of CIB1 delineates a new family of EF-hand-containing proteins. J.Biol.Chem. 2005; 280:8407–8415. [PubMed: 15574431]
15. Huang H, Vogel HJ. Structural Basis for the Activation of Platelet Integrin alphaIIbbeta3 by Calcium- and Integrin-Binding Protein 1. J Am Chem Soc. 2012; 134:3864–3872. [PubMed: 22283712]
16. Yamniuk AP, Anderson KL, Fraser ME, Vogel HJ. Auxiliary Ca2+ binding sites can influence the structure of CIB1. Protein Sci. 2009; 18:1128–1134. [PubMed: 19388079]
17. Yamniuk AP, Nguyen LT, Hoang TT, Vogel HJ. Metal ion binding properties and conformational states of calcium- and integrin-binding protein. Biochemistry. 2004; 43:2558–2568. [PubMed: 14992593]
18. Barry WT, Boudignon-Proudhon C, Shock DD, McFadden A, Weiss JM, Sondek J, Parise LV. Molecular basis of CIB binding to the integrin alpha IIb cytoplasmic domain. J.Biol.Chem. 2002; 277:28877–28883. [PubMed: 12023286]
19. Yuan W, Leisner TM, McFadden AW, Wang Z, Larson MK, Clark S, Boudignon-Proudhon C, Lam SC, Parise LV. CIB1 is an endogenous inhibitor of agonist-induced integrin alphaIIbbeta3 activation. J.Cell Biol. 2006; 172:169–175. [PubMed: 16418530]
20. Naik MU, Naik UP. Calcium-and integrin-binding protein regulates focal adhesion kinase activity during platelet spreading on immobilized fibrinogen. Blood. 2003; 102:3629–3636. [PubMed: 12881299]
21. Naik UP, Naik MU. Association of CIB with GPIIb/IIIa during outside-in signaling is required for platelet spreading on fibrinogen. Blood. 2003; 102:1355–1362. [PubMed: 12714504]
22. Kauselmann G, Weiler M, Wulff P, Jessberger S, Konietzko U, Scafidi J, Staubli U, Bereiter-Hahn J, Strebhardt K, Kuhl D. The polo-like protein kinases Fnk and Snk associate with a Ca(2+)- and integrin-binding protein and are regulated dynamically with synaptic plasticity. EMBO J. 1999; 18:5528–5539. [PubMed: 10523297]
23. Leisner TM, Liu M, Jaffer ZM, Chernoff J, Parise LV. Essential role of CIB1 in regulating PAK1 activation and cell migration. J.Cell Biol. 2005; 170:465–476. [PubMed: 16061695]
24. Yuan W, Leisner TM, McFadden AW, Clark S, Hiller S, Maeda N, O'Brien DA, Parise LV. CIB1 is essential for mouse spermatogenesis. Mol.Cell Biol. 2006; 26:8507–8514. [PubMed: 16982698]
25. Denofrio JC, Yuan W, Temple BR, Gentry HR, Parise LV. Characterization of calcium- and integrin-binding protein 1 (CIB1) knockout platelets: potential compensation by CIB family members. Thromb Haemost. 2008; 100:847–856. [PubMed: 18989529]
26. Heineke J, Auger-Messier M, Correll RN, Xu J, Benard MJ, Yuan W, Drexler H, Parise LV, Molkentin JD. CIB1 is a regulator of pathological cardiac hypertrophy. Nat Med. 2010; 16:872–879. [PubMed: 20639889]
27. Zayed MA, Yuan W, Chalothorn D, Faber JE, Parise LV. Tumor growth and angiogenesis is impaired in CIB1 knockout mice. J Angiogenes Res. 2010; 2:17. [PubMed: 20804551]
28. Zayed MA, Yuan W, Leisner TM, Chalothorn D, McFadden AW, Schaller MD, Hartnett ME, Faber JE, Parise LV. CIB1 regulates endothelial cells and ischemia-induced pathological and adaptive angiogenesis. Circ Res. 2007; 101:1185–1193. [PubMed: 17975111]

29. Hwang PM, Vogel HJ. Structures of the platelet calcium- and integrin-binding protein and the alphaIIb-integrin cytoplasmic domain suggest a mechanism for calcium-regulated recognition; homology modelling and NMR studies. J Mol Recognit. 2000; 13:83–92. [PubMed: 10822252]
30. Roy A, Kucukural A, Zhang Y. I-TASSER: a unified platform for automated protein structure and function prediction. Nat Protoc. 2010; 5:725–738. [PubMed: 20360767]
31. Yang J, Ma YQ, Page RC, Misra S, Plow EF, Qin J. Structure of an integrin alphaIIb beta3 transmembrane-cytoplasmic heterocomplex provides insight into integrin activation. Proc Natl Acad Sci U S A. 2009; 106:17729–17734. [PubMed: 19805198]
32. Schrodinger, LLC. The PyMOL Molecular Graphics System. Version 1.4.1. 2010.
33. Dagliyan O, Proctor EA, D'Auria KM, Ding F, Dokholyan NV. Structural and dynamic determinants of protein-peptide recognition. Structure. 2011; 19:18–731845.
34. Yin S, Biedermannova L, Vondrasek J, Dokholyan NV. MedusaScore: an accurate force field-based scoring function for virtual drug screening. J Chem Inf Model. 2008; 48:1656–1662. [PubMed: 18672869]
35. Ding F, Yin S, Dokholyan NV. Rapid flexible docking using a stochastic rotamer library of ligands. J Chem Inf Model. 2010; 50:1623–1632. [PubMed: 20712341]
36. Yamniuk AP, Ishida H, Vogel HJ. The interaction between calcium-and integrin-binding protein 1 and the alphaIIb integrin cytoplasmic domain involves a novel C-terminal displacement mechanism. J Biol Chem. 2006; 281:26455–26464. [PubMed: 16825200]
37. Huang H, Ishida H, Yamniuk AP, Vogel HJ. Solution structures of Ca2+-CIB1 and Mg2+-CIB1 and their interactions with the platelet integrin alphaIIb cytoplasmic domain. J Biol Chem. 2011; 286:17181–17192. [PubMed: 21388953]
38. Haas TA, Taherian A, Berry T, Ma X. Identification of residues of functional importance within the central turn motifs present in the cytoplasmic tails of integrin alphaIIb and alphaV subunits. Thromb Res. 2008; 122:507–516. [PubMed: 18328539]
39. Vallar L, Melchior C, Plancon S, Drobecq H, Lippens G, Regnault V, Kieffer N. Divalent cations differentially regulate integrin alphaIIb cytoplasmic tail binding to beta3 and to calcium- and integrin-binding protein. J Biol Chem. 1999; 274:17257–17266. [PubMed: 10358085]
40. Yamniuk AP, Vogel HJ. Calcium- and magnesium-dependent interactions between calcium- and integrin-binding protein and the integrin alphaIIb cytoplasmic domain. Protein Sci. 2005; 14:1429–1437. [PubMed: 15883187]
41. Holdgate GA. Thermodynamics of binding interactions in the rational drug design process. Expert Opinion on Drug Discovery. 2007; 2:1103–1114. [PubMed: 23484875]
42. Wimley WC, White SH. Experimentally determined hydrophobicity scale for proteins at membrane interfaces. Nat Struct Biol. 1996; 3:842–848. [PubMed: 8836100]
43. Proctor EA, Yin S, Tropsha A, Dokholyan NV. Discrete molecular dynamics distinguishes nativelike binding poses from decoys in difficult targets. Biophys J. 2012; 102:144–151. [PubMed: 22225808]
44. Yamniuk AP, Gifford JL, Linse S, Vogel HJ. Effects of metal-binding loop mutations on ligand binding to calcium- and integrin-binding protein 1. Evolution of the EF-hand? Biochemistry. 2008; 47:1696–1707. [PubMed: 18197701]
45. Huang H, Bogstie JN, Vogel HJ. Biophysical and structural studies of the human calcium- and integrin-binding protein family: understanding their functional similarities and differences. Biochem Cell Biol. 2012; 90:646–656. [PubMed: 22779914]
46. Hager M, Bigotti MG, Meszaros R, Carmignac V, Holmberg J, Allamand V, Akerlund M, Kalamajski S, Brancaccio A, Mayer U, Durbeej M. Cib2 binds integrin alpha7Bbeta1D and is reduced in laminin alpha2 chain-deficient muscular dystrophy. J Biol Chem. 2008; 283:24760–24769. [PubMed: 18611855]
47. Leisner TM, Moran C, Holly SP, Parise LV. CIB1 prevents nuclear GAPDH accumulation and non-apoptotic tumor cell death via AKT and ERK signaling. Oncogene. 2012

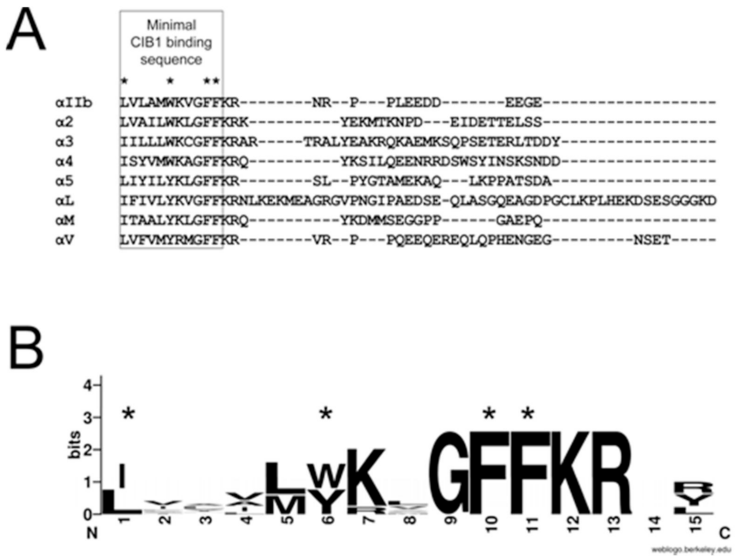

Figure 1.

A) Sequence alignment of select α-integrin tails. The minimum CIB1 binding sequence of integrin αIIb is boxed. Asterisks denote residues in αIIb that are critical for binding to CIB1. B) The consensus logo (generated at http://weblogo.berkeley.edu/), where bits indicate the level of conservation at a position, and letter size indicates the frequency of observing a given residue at a given position.

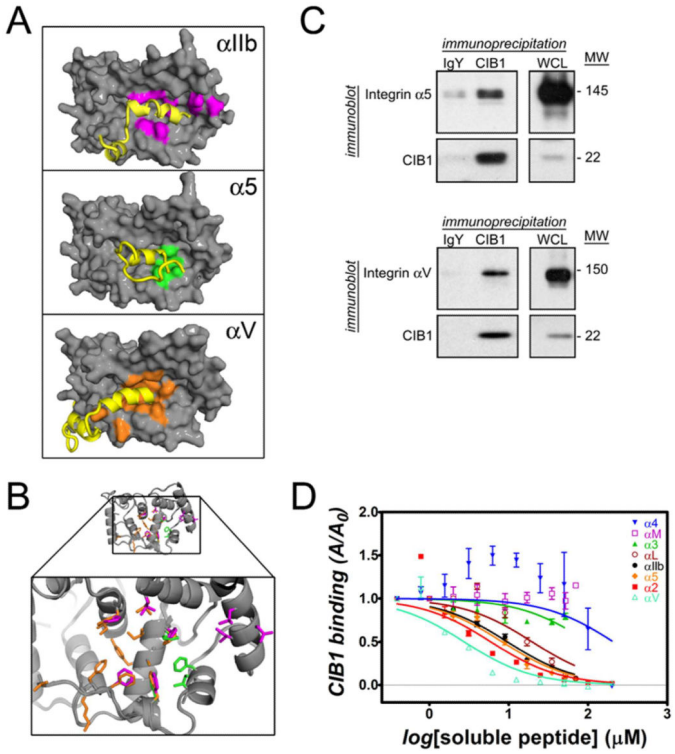

Figure 2.

α-integrin binding site of CIB1. A) Lowest energy structures from molecular docking of α-integrin peptides (yellow cartoons) to CIB1 gray surface. Integrin peptide is indicated in each panel. Residues close enough to contact each peptide are colored on CIB1 surface model. B) Overlay and close-up of integrin-binding residues on CIB1 determined from docking with αIIb (magenta sticks), α5 (green sticks), and αV (orange sticks). C) Immunoprecipitates and whole cell lysates (WCL) from HEK293T cells overexpressing either integrin α5 or αV were lysed and immunoprecipited with either control IgY or anti-CIB1 IgY, and immunoblotted with anti-integrin α5 (upper) or anti-integrin αV (lower), while CIB1 was detected by immunoblotting with an anti-CIB1 antibody. Irrelevant lanes between the immunoprecipitate and WCL lanes were excluded by cropping the images. D) Competitive inhibition binding assays were used to test the binding of CIB1 to eight α-integrin tail peptides. CIB1 binding (y-axis), as measured by absorbance of OPD (*o*-phenylenediamine) at 490 nm, and normalized to A_{490} at the lowest peptide concentration (A_0) is compared to increasing concentrations of a given solution-phase α-integrin peptide (x-axis). Data points represent mean ± SEM (N=2), and fit with a dose-response curve.

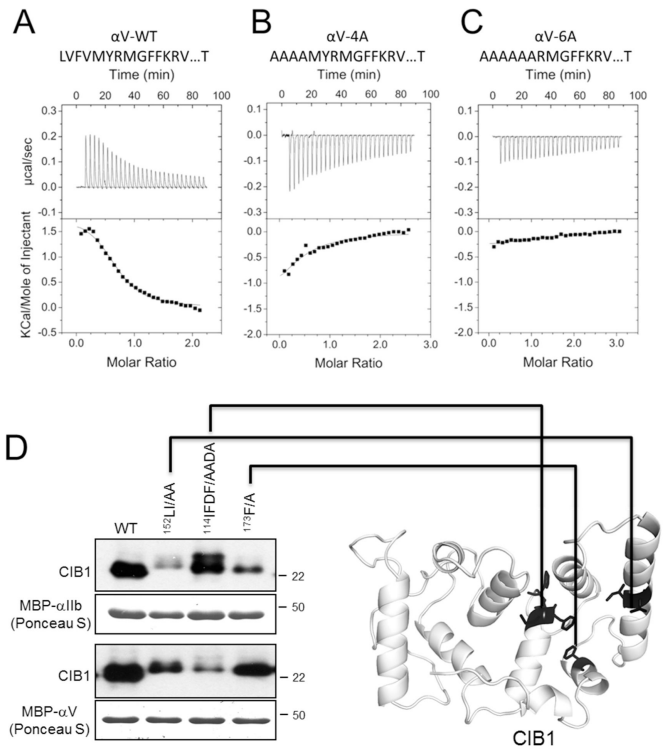

Figure 3.

Validation of interaction sites predicted by DMD. Isotherms (upper) and integrated peaks fit with one site binding model (lower) of A) αV-WT, B) αV-4A, and C) αV-6A. Data of αV-4A and αV-6A do not reasonably fit any standard binding models. D) CIB1 co-precipitation with MBP-αIIb CT and MBP-αV CT. Various CIB1 mutants, indicated above the lanes and highlighted (black) on the structure to the right, were tested for their ability to bind to α-integrin CTs.

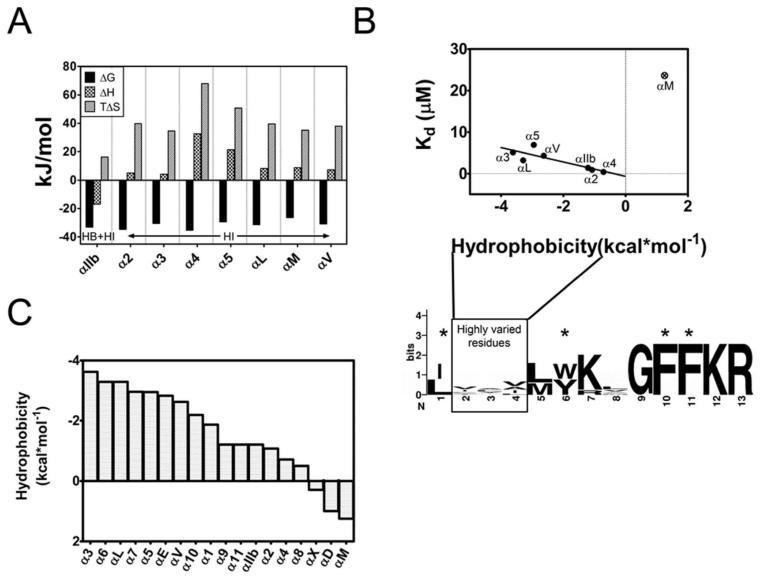

Figure 4.

CIB1 binds to α-integrin CTs through hydrophobic interactions. A) Thermodynamic profiles of CIB1 binding to α-integrins. The free energy ΔG (solid), enthalpy ΔH (checkered), and entropy TΔS (shaded) are plotted for CIB1 binding to the α-integrin CTs shown on the x-axis. The thermodynamic profiles indicate which types of interactions, HB (hydrogen-bonding) or HI (hydrophobic interactions) drive binding. B) N-terminal hydrophobicity of α-integrin CT peptides correlates to CIB1 binding affinity. The CIB1 binding affinity of each α-integrin CT as determined by ITC (y-axis) is compared to the total hydrophobicity of the region indicated in the consensus logo below plot (residues 2-4) of each peptide (●). Data were fit with a linear regression model ($R^2 = 0.72$). The value of αM (⊗) was excluded from the regression as an outlier using the ROUT method of Graphpad Prism 5 with threshold Q = 1.0%. C) Hydrophobicity of residues 2-4 of each α-integrin CT peptide ranked in order of most hydrophobic to least.

Table 1

ITC of CIB1 and α-integrin cytoplasmic tail peptides. Representative titration isotherms are shown in Fig. S2. Errors shown are from fitting the ITC data to a one-site model. Errors are not shown for TΔS or ΔG as those are calculated values.

Integrin	N	K_d (μM)	ΔH (kJ/mol)	TΔS (kJ/mol)	ΔG (kJ/mol)
αIIb	0.9 ± 0.0	1.4 ± 0.1	−16.4 ± 0.1	17.1	−33.4
αIIb[a]	1.2 ± 0.0	3.1 ± 1.8	−34.1 ± 2.2	−2.4	−31.7
α2	1.1 ± 0.0	0.9 ± 0.3	5.0 ± 0.2	39.7	−34.6
α3	1.0 ± 0.0	5.1 ± 1.0	4.2 ± 0.1	34.6	−30.4
α4[a]	0.8 ± 0.0	0.4 ± 0.1	32.7 ± 0.5	67.9	−35.2
α5	0.9 ± 0.0	6.9 ± 0.4	21.4 ± 0.3	50.7	−29.3
αL	1.1 ± 0.0	3.2 ± 0.6	8.2 ± 0.4	39.5	−31.3
αM	1.1 ± 0.0	23.6 ± 1.4	8.8 ± 0.2	35.2	−26.4
αV	0.9 ± 0.0	4.3 ± 0.9	7.3 ± 0.4	38.0	−30.7
αV-4A[b]	N.D.	>100 μM	N.D.	N.D.	N.D.
αV-6A[b]	N.D.	>>100 μM	N.D.	N.D.	N.D.

[a] ITC of α4 was performed in ITC buffer without any NaCl due to peptide solubility issues. αIIb binding to CIB1 was also tested in the absence of NaCl with insignificant effects on the binding affinity. However, the thermodynamic properties suggest a change in the mechanism of binding.

[b] N.D. = Not determinable. The CIB1 binding affinities of these ligands must be greater than the upper limit of detection for ITC (100 μM).